IL-21 and CD40L synergistically promote plasma cell differentiation through upregulation of Blimp-1 in human B cells[1]

B. Belinda Ding[*,2], **Enguang Bi**[*,2], **Hongshan Chen**[*], **J. Jessica Yu**[*], and **B. Hilda Ye**[*,†]
[*]Department of Cell Biology, Albert Einstein College of Medicine, Bronx, NY 10461, USA

Abstract

After undergoing Ig somatic hypermutation and antigen selection, germinal center (GC) B cells terminally differentiate into either memory or plasma cells (PCs). It is known that the CD40L and IL-21/STAT3 signaling pathways play critical roles in this process, yet it is unclear how the B cell transcription program interprets and integrates these two types of T cell derived signals. In this study, we characterized the role of STAT3 in the GC-associated PC differentiation using purified human tonsillar GC B cells and a GC B cell-like cell line. When primary GC B cells were cultured under PC differentiation condition, STAT3 inhibition by AG490 prevented the transition from GC centrocytes to pre-plasmablast (pre-PB) suggesting that STAT3 is required for the initiation of PC development. In a GC B cell-like human B cell line, although IL-21 alone can induce low-level Blimp-1 expression, maximum Blimp-1 upregulation and optimal PC differentiation required both IL-21 and CD40L. CD40L, while having no effect on Blimp-1 as a single agent, greatly augmented the amplitude and duration of IL-21 triggered Jak-STAT3 signaling. In the human *PRDM1* locus, CD40L treatment enhanced the ability of STAT3 to upregulate Blimp-1 by removing BCL6, a potent inhibitor of Blimp-1 expression, from a shared BCL6/STAT3 site in intron 3. Thus, IL-21 and CD40L collaborate through at least two distinct mechanisms to synergistically promote Blimp-1 activation and PC differentiation.

Introduction

A key aspect of the humoral immune response is terminal differentiation of activated B cells into antibody secreting plasma cells (PCs). Although Blimp-1 upregulation is necessary and sufficient for the appearance of functional PCs (1), PC differentiation starts prior to Blimp-1 activation and can give rise to the so-called "pre-plasmablast" (Pre-PB) in a Blimp-1-independent manner (2, 3). The pre-PB is a CD138 (Syndecan) –negative cell characterized by low level Ig secretion, compromised Pax5 function, and expression of two PC-associated transcription factors, XBP-1 and IRF4 (2, 3). Believed to be developmentally plastic, pre-PB represents a transient and yet important step in PC differentiation. The initial identification and functional characterization of pre-PB took advantage of an elegant Blimp-1 knock-in mouse model (3). In human, existence of the pre-PB has not been rigorously defined. Nevertheless, in both mouse and human, the term plasmablast is reserved for the dividing PC precursors that express CD138 (Syndecan) and bone marrow homing receptors, including CD44, VLA-4, and LFA-1 (2, 4). One of the goals of the current study is to better define human pre-PB in molecular terms.

[†]CORRESPONDENCE: B. Hilda Ye, Department of Cell Biology, Albert Einstein College of Medicine, 1300 Morris Park Avenue, Bronx, NY 10461, Phone: (718) 430-3339, Fax: (718) 430-8574, hilda.ye@einstein.yu.edu.
[2]These two authors contributed equally to this work.

In vivo, PCs can be generated through the extra follicular route as well as the GC response (1). While both pathways share a strict requirement for IRF4 and Blimp-1, the GC-associated PC differentiation has additional requirements and is subject to more elaborate control. Presumably, this is due to the fact that only the affinity matured GC B cells can give rise to long-lived PCs as well as memory B cells (1, 2) so that, if dysregulated, these GC offspring will cause more damage to the organism compared to the short-lived extrafollicular antibody response (5). Three major differences exist between the two pathways of PC development. First of all, STAT3 is dispensable for T cell-independent, extrafollicular Ab response but crucial for post-GC differentiation of IgG PCs (6). Nevertheless, the reason for this pathway-specific function of STAT3 is unknown; the specific stage of PC development that requires STAT3 function is also not defined. Secondly, initiation of PC differentiation within a GC B cell requires the downregulation of BCL6, a transcriptional repressor that inhibits the expression of three critical transcription factors for PC development, e.g., STAT3, IRF4, and Blimp-1 (7–11). This BCL6-imposed barrier for PC differentiation is much lower for the extrafollicular pathways since naïve B cells have very little BCL6 protein (12). Lastly, unique to the GC-associated PC development is the role played by follicular T helper (Tfh) cells, which regulate all aspects of the GC response (13). Recent multi-photon microscopy studies have suggested that GC B cells compete for limited Tfh help signals within the GC light zone (14, 15). A combination of this cognate B-T interaction and a direct contribution from the follicular dendritic cells (FDCs) (16) presumably provides the cellular basis for positive selection that licenses affinity matured GC B cells into the long-lived PC pools.

Tfh cells provide help to B cells through a variety of molecules that regulate GC initiation, maintenance, and post-GC B cell differentiation (17). In the light zone of established GCs, a major Tfh-derived help signal is delivered through CD40 ligation. Direct T-B contact in the GC light zone results in CD40L-CD40 engagement, which triggers NF-κB activation and IRF4 upregulation within the B cell (18). IRF4 in turn downregulates BCL6 thereby creating a permissible state for post-GC differentiation (18). Tfh cells also regulate Ig class-switching and B cell maturation through several cytokines, including IFNγ, IL-4, IL-10, IL-13, and IL-21. Recent studies have particularly focused on IL-21, a type I cytokine that has been recognized as the most potent driver of B cell terminal differentiation and acts directly on B cells to control GC formation and antibody production (19, 20). Of note, all three major cytokines involved in PC development, IL-21, IL-6, and IL-10, share the ability to activate STAT3. As pointed out above, although STAT3 is known to play a critical role in post-GC PC differentiation, the timing of STAT3 requirement in the PC development process has not been defined. It is also not clear if and how STAT3 activation integrates other Tfh signals such as CD40L.

In this study, we used primary tonsillar GC B cells and a GC B cell-like cell line system to characterize the signaling events leading to STAT3 activation and the subsequent changes in target gene expression and B cell phenotype. Our results confirm a number of previous reports but also provide novel insights regarding the timing of STAT3 requirement, the nature of cooperativity between CD40L and IL-21 signaling in GB B cells, and the importance of competitive binding between BCL6 and STAT3 to the intron 3 site in the human *PRDM1* locus. The cell line-based PC differentiation system we described here is remarkably robust and amenable to detailed biochemical analysis and somatic cell genetics. It should serve as a valuable tool for future studies, in particular, with respect to the phenotypic transition from GC B cells to plasma cell precursors.

Materials and Methods

Purification of tonsillar centroblast B cells

Human tonsils were obtained as discarded material from routine tonsillectomies with approval of the Institutional Review Boards of AECOM and Montefiore Medical Center in accordance with Helsinki protocols. The FDC-like HK cells and the stable CD40L-CD8-transfected J558 cell line have been previously described (21, 22). GC centroblasts were purified from freshly obtained tonsillectomy specimens by one step, magnetic cell separation based on CD77 as previously described (11). Briefly, finely minced tonsillar tissue in ice-cold RPMI medium was passed through a 70 μM Nylon filter (BD Falcon). The cleared cell suspension was spun over Histopaque 1077 (Sigma-Aldrich) to obtain mono-nuclear cells. The recovered cells were washed twice with PBS before sequential staining with 3 antibodies. First, cells were suspended in 500 ul of PBS+ 4% FBS, and incubated with anti-CD77 rat IgM antibodies (Beckman Coulter, clone 38-13, 15μl per 1×10^8 cells). The stained cells were washed once with PBS, and resuspended again in 500 ul of PBS+ 4% FBS, to which mouse anti-rat IgM antibodies (BD Biosciences, Cat. 553887) was added (7 ul per 1×10^8 cells). After incubation, the stained cells were washed, resuspended as before, and stained with rat anti-mouse IgG1 microbeads (Miltenyi Biotec, Cat. 130-047-101, 17 ul per 1×10^8 cells). All antibody binding steps were carried out on ice for 10–20 minutes. Finally, the stained cells were subject to magnetic cell separation according to the manufacturer's protocol. To isolate native B cells from tonsils, a two-step antibody staining procedure was used which involved the use of FITC labeled anti-human IgD in the first step and anti-FITC microbeads in the second step. Based on flow cytometry analysis, the purity of isolated cells is typically more than 95% (Fig. 1*A*).

Flow cytometry

Cells were washed in cold PBS containing 5% FCS and stained with the following antibodies according to standard techniques: FITC-anti-human CD20 (BD Cat. 555778), PE-anti-human CD38 (BD Cat. 555460), FITC-anti-human CD138 (BD Cat. 552723), PE-mouse IgG1κisotype control (BD Cat. 555749), APC-anti-CD44 (BD Cat. 559942), APC-anti-CD27 (BD Cat. 558664), FITC-anti-human HLA-DR (BD 555560). Flow cytometry was performed using a FACScan (BD) and the data were analyzed using FlowJo software (Tree Star, Inc.).

In vitro differentiation culture

To differentiate primary GC B cells, purified centroblasts were plated at a density of 6×10^5/ml over 3×10^3 adherent HK cells in a single well of a 24-well plate. Supernatants from the CD40L-CD8 secreting J558 cells were used in a 1:250 dilution in combination with recombinant human IL-2 (25 ng/ml) and IL-4 (50 ng/ml) (PeproTech, Cat. 200-02 and 200-04). When needed, recombinant human IL-21 (50 ng/ml) (PeproTech, Cat. 200-21) was also added to the culture. During the next two weeks, aliquots of cells and/or culture supernatants were removed for analysis of protein and RNA expression, cell surface marker change, and Ig secretion. As previously reported, purified GC B cells exhibited significant cell death *in vitro*, especially during the first 4 days of culture even in the presence of CD40L (23, 24). To address this issue, once every 4 days, live cells were enriched by low speed centrifugation and reseeded in half of the original volume. The GC B cell-like diffuse large B cell lymphoma cell line, Ly7, was maintained in IMDM medium with 10% FBS. To establish the NIH 3T3 cell line stably expressing the mouse CD40L, 3T3 cells were transfected with a mCD40L-expressing pcDNA4/TO vector, followed by Zeocin selection. Surface expression of mCD40L was validated by flow cytometry analysis. To induce plasma cell differentiation in Ly7, 5×10^5 cells were seeded in 1 ml into a single well of 12-well dish. Recombinant human IL-21 was added to 100 ng/ml final concentration. Under the

costimulation condition, Ly7 cells were seeded into a 12-well that contained 4×10^4 adherent 3T3-vector or 3T3-CD40L cells. In the following 10 days, B cells in differentiation medium were split once every 3 days and plated on new feeder cells. Changes in gene expression, cell surface phenotype, and Ig secretion status were tracked during the two weeks of a differentiation experiment.

siRNA-mediated STAT3 knock-down

The sequence of STAT3-specific siRNA and the procedure used to knock-down STAT3 in human B cell lines have been described (7). Briefly, transient transfections were performed with the Nucleofector Kit T and program G16 (Amaxa Biosystems). Ten micrograms of control or STAT3-directed siRNA oligos were used in each transfection of 5–10 million cells.

Construction of Blimp-1 Luciferase Reporters and Reporter Assays in Ly7 cells

A 1.71 kb genomic DNA fragment containing the intron 3 BCL6/STAT3 site was PCR-amplified from the BAC clone RP11-48H3 using Sal I restriction site-adapted PCR primers 5′ ACGCGTCGACGTCGGCCATAGCGGCCGCGGAATCCTTGAATAAAACACTGGATT AGC (Forward) and 5′ ACGCGTCGACGTCGGCCATAGCGGCCGCGGAAGCAGAATGAAGAATTTGA AGTTTGT. The PCR products were Sal I-digested and inserted into similarly digested Blimp-1 Luciferase reporter containing the 1.67 kb 5′ promoter sequence (25). This resulted in insertion of the 1.71 kb intron 3 fragment downstream of the Luciferase coding region. The composite BCL6/STAT3 site, TTCCTGGAA, was subsequently mutated to TCTCTGAGA by site-directed mutagenesis using the QuikChange II kit (Stratagene). All constructs were sequence-verified. For reporter assays, 6 million Ly7 cells were transfected using the Nucleofector Kit T and program G16 with 1 pmol of the Luciferase reporters (4.5–5.7 ug) plus 3 ug of a β-gal control plasmid. After overnight incubation, transfected cells were either left untreated or subject to IL-21/CD40L costimulation for 44 h. Luciferase activities were measured with the Luciferase Assay System (Promega) and normalized by control readings from the βgal assays.

Quantitative RT-PCR (qRT-PCR) and Western blotting

Western blotting and qRT-PCR were performed using standard techniques as previously described (26). Primers used for qRT-PCR are listed in Supplementary Table 1. Primary antibodies used for Western Blot analysis were purchased from Santa Cruz Biotechnology for BCL6 (sc-858), Blimp-1 (sc-47732), IRF4 (sc-6059), Pax5 (sc-1974), STAT3 (sc-8019 and sc-482), GAPDH (sc-25778), from Cell Signaling Technology for Jak3 (#3775), STAT1 (#9172), PY-Jak1 (#3331), PY-STAT1 (#9171), PY-STAT3 (#9131), PS-STAT3 (#9123), from BD Pharmingen for IL-21R (560264), from Invitrogen Life Science for PY-Jak2 (44-426G), and from Calbiochem for MTA3 (IM1012). Mum1 mAb (IgG1 clone 2H9) was obtained from Dr. Falini at University of Perugia, Italy.

ELISA

Levels of secreted antibodies in the culture supernatants were measured using Human IgM and IgG ELISA Quantitation Kits (Bethyl Laboratories, Inc., Cat. E80-100 and E80-104). Serial dilutions and standard curves were performed to calculate Ab concentrations based on ½ Vmax using GraphPad Prism.

Quantitative Chromatin Immunoprecipitation (qChIP)

We used a previously described protocol for locus-specific ChIP in lymphoma cell lines and quantitative measurement of enriched DNA material (26). The same BCL6 and STAT3 polyclonal antibodies used for Western Blot were used in these experiments. The primers used for qPCR are listed in Supplementary Table 1.

Results

Jak/STAT activity is required for the centrocyte to pre-PB transition in an in vitro PC differentiation system

To study the timing and consequence of STAT3 activation with respect to PC differentiation stages, we turned to a previously described *in vitro* differentiation system for tonsillar GC B cells (27–29). Specifically, GC centroblasts (CBs) were purified from tonsils using CD77-based magnetic beads enrichment and subsequently cultured on the HK feeder cell line in the presence of soluble CD40L, IL-2, and IL-4. As shown in Fig. 1, robust plasma cell differentiation was induced in 10–12 days based on gradual changes in surface phenotype, transcription factor expression, and Ig secretion capability. Specifically, freshly isolated GC centroblasts had high levels of BCL6 and Pax5, both of which ceased expression rapidly in the differentiation medium and were replaced by transcription factors associated with PC differentiation after a week, namely Tyr705 phosphorylated STAT3 (PY-STAT3), Blimp-1, and IRF4 (Fig. 1*B*). Expression of IRF4 was also examined by the Mum1 Ab, which recognizes a conformational epitope preferentially expressed by nuclear localized IRF4 (30). After 1 week, Ig secretion started to increase steadily reaching 100 μg IgM per 10^6 cells per ml on day 11 (Fig. 1*C*). Although the trend for IgG Ab was the same, the levels were ~1000 times lower indicating inefficient class switching *in vitro.* We also examined B cell phenotype changes based on surface marker expression. As previously reported, freshly purified human GC centroblasts were CD20^{hi}CD38^{hi}. During the next 10 days, two other phenotypes gradually emerged under our culture condition: CD20$^+$CD38$^+$ and CD20$^-$CD38$^+$, which are referred to as centrocytes (CCs) and plasmablasts (PBs), respectively, based on previous reports (27–29) (Fig. 1*A*). Although culture cocktails that include CD40L are reported to produce CD20$^+$CD38$^-$ memory B cells, we rarely detected these cells possibly due to suboptimal CD40L stimulation in our cultures. Interestingly, in addition to the CC and PB subsets, we also observed a CD20$^-$CD38$^-$ population that appears to represent an intermediate phenotype. This population was most prominent on Day 7 as the CC fraction started to decrease, and began to contract on Day 10 when the PB subset started to dominate the culture (Fig. 1*A*).

To examine the role of Jak/STAT signaling in this system, we added the Jak inhibitor, AG490, to parallel cultures. In some experiments, the effect of IL-21 was also tested. In the presence of AG490, the CB to CC transition was not affected, an observation consistent with our previous report that all tonsillar CBs are STAT3-negative (7). However, AG490 substantially blocked the transition from CC to the CD20$^-$CD38$^-$ population on Day 7 leading to a drastic reduction of the CD20$^-$CD38$^+$ PBs in later stages of the culture, such as shown on Day 10. Consistent with the PC promoting activity of the IL-21/Jak/STAT3 axis, Ig secretion was also reduced by AG490 but notably enhanced by IL-21 (Fig. 1*C*). This AG490 effect not only confirms our interpretation that the CD20$^-$CD38$^-$ population is the predecessor to the CD20$^-$CD38$^+$ PBs, it also suggests that Jak/STAT activity is required for CC to acquire this next, more mature phenotype (CD20$^-$CD38$^-$). We also looked for gene expression changes associated with the transition from CD20$^+$CD38$^+$ to CD20$^-$CD38$^-$ phenotype. Quantitative RT-PCR (qRT-PCR) experiments revealed that between Day 6 and Day 8 when the CD20$^-$CD38$^-$ fraction started to appear, there was an abrupt increase in both *Jak3* and *IRF4* mRNA; more importantly, such increase was delayed and reduced in

AG490 treated cultures (Fig. 1*D*). Of note, Jak3 is a well-known STAT3 target gene (ref (31) and data not shown), while upregulation of IRF4 was previously reported to coincide with the appearance of pre-PB in mouse B cells (2).

A cell line based system to study post-GC plasma cell differentiation

Although our experiments with purified human GC B cells were very informative, we needed an experimental system that was more amenable to molecular and biochemical analyses. To this end, we screened a panel of GC B cell-like diffuse large B cell lymphoma (GCB-DLBCL) cell lines for their ability to undergo PC differentiation under costimulation by IL-21 and cell membrane-bound CD40L. Among the 3 responsive cell lines identified, including Ly7, Ly8, and SuDHL6, Ly7 was the most responsive and was used for the rest of our study. Unstimulated Ly7 cells and Ly7 cells exposed to the control 3T3 feeder for less than 1 week displayed a CD20$^+$CD38$^+$ (CB/CC) phenotype (Fig. 2*A* and not shown). This phenotype was not altered when Ly7 cells were subjected to either IL-21 or 3T3-CD40L single treatment for 1 week. In contrast, in the IL-21/CD40L costimulation culture, only 19% of the cells remained CD20$^+$CD38$^+$ while 57% adopted a CD20$^-$CD38$^-$ phenotype (Pre-PB like) and 23% were CD20$^+$CD38$^-$ (PB-like) (Fig. 2*A*, top panel). After 2-weeks stimulation, 21% of the cells exposed to control 3T3 feeder cells and nearly all the cells stimulated with 3T3-CD40L had become CD20$^-$CD38$^-$(Pre-PB). However, CD20$^-$CD38$^+$ cells (PBs) were only seen in the IL-21 culture and more prominently detected under IL-21/ CD40L costimulation condition (Fig. 2*A*, bottom panel). The CD20$^-$CD38$^+$ PBs were also positive for CD27 but negative for Syndecan/CD138 (not shown). Consistent with the notion that the CD20$^-$CD38$^-$ subset has the pre-PB phenotype (limited Ig secretion capacity) while the CD20$^-$CD38$^+$ cells possess PB-like features (better Ig producers), ELISA revealed that IL-21 alone had a modest stimulatory effect on IgM and IgG production, which was most obvious after 2 weeks of treatment. Cells treated with CD40L alone also produced low levels of IgM and IgG. The highest levels of IgM and IgG were detected with IL-21/CD40L costimulation, reaching ~12 μg/ml and 170 ng/ml, respectively, after 2 weeks of culture. This result indicates that the Ly7 cell line supports the synergistic effect of IL-21 and CD40L previously reported in primary mouse and human B cells. It is of note that under the costimulation condition, the gradual increase in IgG titers closely paralleled that of IgM suggesting a lack of progressive class switching. Two other GCB-DLBCL cell lines, Ly8 and SuDHL6, also responded to the costimulation with similar but milder changes in cell surface CD20/CD38 expression and Ig secretion (not shown).

IL-21 and CD40L synergistically induce Blimp-1 expression in a STAT3-dependent manner

Numerous *in vivo* studies have shown that nearly all factors important for the early stage of PC differentiation exert their effect through activation and/or maintenance of Blimp-1, the PC master regulator encoded by the *PRDM1* gene. We therefore sought to compare IL-21 and CD40L in their abilities to activate Blimp-1 in differentiating Ly7 cells. Unstimulated Ly7 cells displayed a typical GC B cell phenotype: BCL6, MTA3, and Pax5 high, STAT3 and IRF4 low, PY-STAT3 and Blimp-1 negative (Fig. 3*A*, lane 1). IL-21 alone activated PY-STAT1/3, which was accompanied by the appearance of PY-Jak1 and elevated total Jak3 (lane 2), but not PY-STAT5/6 (not shown). Interestingly, IL-21 as a single agent also upregulated IRF4 moderately and weakly induced Blimp-1 (Fig. 3*A*, comparing lane 2 to 1 and lane 5 to 3; a more typical Blimp-1 response to IL-21 is seen in Fig. 3*B*, lane 2 compared to lane 1). Although results shown in Figure 1*A* are after 46 h stimulation, IL-21-triggered increase in Jak3, STAT3, IRF4, and Blimp-1 was detected as early as 24 h (Supplementary Fig. 1). CD40L alone had no effect on Blimp-1 although it increased IRF4 and Jak3 while reducing the expression of BCL6 and PY-Jak2 (Fig. 3*A*, comparing lane 4 to lane 3). Most importantly, we observed a substantial synergism between IL-21 and CD40L in upregulating Blimp-1 (comparing lane 6 to lane 4 and 5). Similar cooperative effects were

also observed for PY-Jak1, PY-STAT1/3, and total STAT3. The influence from IL-21 and CD40L on IRF4 and Jak3 appeared to be additive. Pax5 and MTA3 levels remained fairly constant through all treatments with the exception of a mild MTA3 reduction under the costimulation condition (Fig. 3*A*, lane 6).

Since both STAT1 and STAT3 were activated following IL-21 stimulation, we used RNA interference to examine the requirement for STAT3 in this system. As shown in Fig. 3*B*, siRNA-mediated STAT3 knock-down (Fig. 3*B*, bottom) markedly reduced the increase in PY-STAT3, IRF4, and most importantly, Blimp-1 in response to IL-21 as well as to the IL-21/CD40L costimulation. This result is consistent with a recent human study showing that STAT3 but not STAT1 is required for long-lived antibody response and IL-21-induced Ig secretion *in vitro* (32). Both Jak1 and Jak3 are known to be critical to the cellular response to IL-21 (33, 34). Using siRNA-mediated Jak3 knock-down, we confirmed that much of the IL-21-associated gene expression changes were also Jak3-dependent (not shown). In addition to confirming a critical role of STAT3 and Jak3 in IL-21-driven PC differentiation, our results also show that in Ly7 cells, the wiring and property of the IL-21R/Jak/STAT pathway are the same as in primary human B cells.

CD40L costimulation altered the dynamics of IL-21R/Jak/STAT3 signaling

The synergism between IL-21 and CD40L in promoting PC development and antibody secretion has been previously reported (35, 36). However, the underlying mechanism has not been examined in great detail. Given the central role of Jak/STAT3 signaling in our experimental system, we analyzed the influence of CD40L/CD40 binding on IL-21R signaling. In a simple setting, Jak/STAT signaling downstream of cytokine receptors features a rapid activation/de-activation cycle (37). This phenomenon was also observed in IL-21 treated Ly7 cells that were pre-exposed to control 3T3 feeder cells. Specifically, the PY-STAT3 signal rose quickly after IL-21 stimulation and plateaued around 30 min to 1 h; by 3 h, it was already reduced to about half of its peak level (Fig. 4*A*, left gel picture and right graph). In comparison, CD40L pre-treatment increased the amplitude of PY-STAT3 response by ~85%. More importantly, the strength of the PY-STAT3 signal remained at near peak-level at 3 h indicating a much sustained response (Fig. 4*A*, right graph, Fig. 4*B* graph). We also examined changes in phospho-Ser727 STAT3 and observed a similar yet milder trend compared to PY-STAT3 (Fig. 4*A*).

We then examined the effect of CD40L-pretreatment on the key components of the IL-21R signaling complex during the first 3 h of IL-21 stimulation. Although CD40L did not change the total IL-21R protein based on Western Blot analysis (Fig. 4*A*), flow cytometry revealed that the surface expression of IL-21R was much higher in CD40L pretreated cells prior to IL-21 exposure (Fig. 4*C*, MFI 20.2 vs 11.9). Interestingly, IL-21 treatment caused a rapid IL-21R down-modulation so that by 1 h, less than 40% of the initial level remained on the cell surface and this amount persisted until at least 3 h (Fig. 4*C*, and data not shown). The same residual amount of IL-21R was detected when IL-21 concentration varied between 20–100 ng/ml and irrespective of CD40L-pretreatment (Fig. 4*D*). Since the CD40L-pretreated cells had higher levels of surface IL-21R prior to IL-21 exposure but retained the same amount of IL-21-resistant receptors on the cell surface, enhanced Jak/STAT signaling in these cells must originate from the internalized IL-21/IL-21R/Jak/STAT complexes within the endocytic compartment.

Collaboration of signals transduced from CD40 and IL-21R on the PRDM1 locus

Since Blimp-1 upregulation epitomized the collaborative effect between CD40L and IL-21, we studied transcription regulation of the *PRDM1* locus. By qRT-PCR analysis, we first confirmed that costimulation with IL-21 and CD40L had the same synergistic effect on

Blimp-1 mRNA as observed on its protein (Fig. 5*A*). Similar synergistic effects were also detected for *Jak3* and *STAT3* mRNA (Supplementary Fig. 2). Using the MatInspector program (38), we identified 3 candidate STAT3 binding sites in the 5′ regulatory region of the human *PRDM1* locus (Fig. 5*B*). Of note, because site B and C are only 147 bp apart, binding to them could not be resolved using PCR-based ChIP analysis. Although all 3 sites can be recognized by STAT3 in *in vitro* binding assays (not shown), activated STAT3 was recruited only to site B/C but not A in Ly7 cells treated with either IL-21 or IL-21 plus CD40L (Fig. 5*C*, top panel, and data not shown). Interestingly, IL-21/CD40L costimulation increased STAT3 occupancy at site B/C by only 30% relative to IL-21 single treatment. Considering the strong and synergistic effect of IL-21 plus CD40L on *Blimp1* mRNA, we reasoned that additional regulatory element(s) must exist in this locus that are more sensitive to the concurrent signaling through IL-21R and CD40. To this end, we examined the high affinity BCL6 binding site in the intron 3 because it is the most critical element mediating the PC inhibitory effect of BCL6 in human B cells (9), whereas it matches perfectly to the canonical STAT3 binding site (39). In untreated Ly7 cells, this site was exclusively occupied by BCL6 (Fig. 5*C*, bottom panel). After 1 h IL-21 stimulation, although the total amount of BCL6 in the cell was not altered (Supplementary Fig. 3*B*), BCL6 binding to this site was reduced by 64% as STAT3 was loaded onto the same site (Fig. 5*C*, middle and bottom panels). Consistent with our observation that CD40L/CD40 engagement did not activate STAT3, CD40L pretreatment did not induce STAT3 binding to any of the STAT3 sites tested; however, it reduced BCL6 binding to the intron 3 site by ~ 30% (Fig. 5*C*, bottom panel); this corresponded to a 50% reduction in cellular BCL6 levels (Supplementary Fig. 3*B*). Presumably, this CD40L effect on BCL6 was the result of NF-κB activation and subsequent IRF4 upregulation (18). Under the costimulation condition, although the total BCL6 protein was not further reduced, BCL6 binding to the intron 3 site was decreased by another 30%; at the same time, STAT3 binding to this site was more than doubled relative to the IL-21 treatment alone (Fig. 5*C*, middle panel). We then turned to transient transfection-based Luciferase reporter assays to address the role of the intron 3 BCL6/STAT3 site in a functional setting. As shown in Figure 5*D*, only the intron 3-containing constructs but not the promoter only reporter responded to IL-21/CD40L costimulation. In addition, in un-stimulated Ly7 cells, the reporter containing the wild type intron 3 sequence (I3-WT) had a significantly lower Luciferase reading compared to the promoter only reporter (Prom), and this difference disappeared when the BCL6/STAT3 composite site was mutated (I3-Mut). This result is consistent with our chromatin IP analysis showing BCL6 occupancy of this site in un-stimulated Ly7 cells (Fig. 5*C*). While the activity of I3-WT more than doubled in response to IL-21/CD40L costimulation, a 40% increase was also observed with the I3-Mut reporter. This is likely due to the remaining STAT-like sites in the 1.7 kb intron 3 sequence. In summary, these data revealed that BCL6 and STAT3 bind in a competitive fashion to the shared *PRDM1* intron 3 site that plays a key role in Blimp-1 upregulation. In addition, the synergistic action of CD40L and IL-21 on Blimp-1 expression is recapitulated by the dynamics of BCL6 and STAT3 recruitment to this intron 3 motif.

Discussion

Although STAT3 has emerged as a key regulator of GC-associated PC development, upstream signaling events leading to its activation and its downstream transcription and cellular effects are incompletely characterized. In this study of human GC B cells, we showed that STAT3 activation is required for activated centrocytes to acquire the CD20⁻CD38⁻ pre-PB phenotype. In addition, we also demonstrate for the first time that concurrent CD40L stimulation potentiates IL-21-driven Blimp-1 upregulation and PC differentiation by altering IL-21R/Jak/STAT3 signaling dynamics and by displacing BCL6 from the shared BCL6/STAT3 site in intron 3 of the *PRDM1* locus (summarized in Fig. 5*E*).

Studies using the Blimp-1-GFP reporter mice showed that PC differentiation begins with the appearance of pre-PBs that are Pax5$^+$IRF4$^+$Blimp-1$^{+/-}$CD138$^-$ (2, 3). Yet, extracellular signals and key transcriptional changes that drive this GC-to-pre-PB transition are not fully understood. We previously reported that in tonsillar GC B cells, the decline in BCL6 is associated with STAT3 activation and upregulation, and that this transient state of STAT3 activity precedes high level Blimp-1 expression (7). Furthermore, B cells with activated STAT3 are only found in the apical light zone, a location rich in FDC and Tfh. From a developmental perspective, these PY-STAT3$^+$ centrocytes should correspond to the pre-PB stage. This notion is supported by three lines of evidences. First, STAT3 provides an activating signal for both IRF4 and Blimp-1 upregulation (Fig. 1*D*, Fig. 3*B*). Second, persistent Jak/STAT activity is required for the appearance of the CD20$^-$CD38$^-$ cells and the CD20$^-$CD38$^+$ PB fractions (Fig. 1*A*), and the ultimate Ig secretion (Fig. 1*C*). Third, David Tarlinton and colleagues have previously reported that IRF4 upregulation marks the emergence of pre-PB in mouse B cells (2), while in our experimental system, IRF4 upregulation coincides with the appearance of the CD20$^-$CD38$^-$fraction. One caveat with experiments based on primary GC B cell cultures is the difficulty to distinguish a primary differentiation effect on centrocytes from a cell proliferation/survival effect on more differentiated cells. Here, the Ly7-based differentiation system offers a unique advantage. Ly7 cells differentiated in a very robust and synchronous manner in response to IL-21/ CD40L costimulation (Fig. 2*A*). And yet, cell proliferation was largely unaltered during the first 4 days based on viable cell count and thymidine incorporation (not shown). Thus, when combined, our data from the primary GC B cell culture and the Ly7 costimulation assays support the notion that STAT3 controls the initiation step of the PC differentiation program by upregulating both IRF4 and Blimp-1. This is to say that in our experimental systems, STAT3 functions upstream of IRF4. This is evidenced by the Jak/STAT requirement in IRF4 upregulation in the primary GC B cell culture and in IL-21 stimulated Ly7 cells (Fig. 1*D* and Fig. 3*B*). In addition, STAT3 was inducibly recruited to the IRF4 promoter region in Ly7 cells treated with IL-21. Furthermore, STAT3 can upregulate IRF4 promoter activity in reporter assays (not shown). All of these observations suggest that IRF4 is a direct target gene of STAT3. In a previous study, forced over-expression of IRF4 was found to upregulate *Blimp-1* mRNA in Ly7 cells (40). In our experiments, however, STAT3 clearly plays a much more important role than IRF4 in driving Blimp-1 upregulation. This is because IL-21 alone can induce low levels of Blimp-1 despite the paradoxical elevation of BCL6 protein, the inhibitor of Blimp-1 (Fig. 3*A*). The IRF4 component of the IL-21 response is unlikely to be the major driver because in cells exposed to CD40L alone, Blimp-1 expression was never detected despite a similar IRF4 increase and the concurrent disappearance of BCL6, a condition that should favor Blimp-1 activation (Fig. 3*A*). Collectively, our results are most consistent with a model in which sustained STAT3 activation driven by concurrent IL-21 and CD40L signals upregulates IRF4, which then downregulates BCL6, thereby enabling maximum STAT3 recruitment to the *PRDM1* locus and high-level Blimp-1 expression (Fig. 5*E*). Given that STAT3 is a direct target gene of BCL6 (7), this model also implicates STAT3, as opposed to IRF4 or Blimp-1, as the most proximal target of BCL6 in its ability to inhibit PC differentiation.

Our results in the current study also have notable implications for how the PC differentiation program might integrate different inputs in the GC microenvironment. FDCs and their associated complement and Fc receptors have long been recognized as important factors for affinity-based section of long-lived PCs (16). The central role played by Tfh cells, however, was only recently proposed. Multi-photon microscopy studies showed that GC B cells loaded with FDC-derived antigens compete for the limited number of Tfh cells in the GC light zone (14, 15). Such observations predict that the BCR affinity-based access to FDC-associated antigen is translated into the amount of MHC-presented peptides to Tfh cells, and hence the difference in receiving proliferation/survival signals (5). A major finding of our

study is that optimal Jak/STAT3 signaling and Blimp-1 upregulation requires concurrent CD40L/CD40 interaction. Incorporating our results into the model above, we would like to further propose that one type of critical T cell help delivered after T-B interaction is via the membrane bound CD40L which, in addition to promoting proliferation/survival, greatly augments the cell signaling and differentiation potential of IL-21 hence facilitating the GC-to-PC phenotypic transition. This key requirement for direct T-B interaction also safeguards against selection of low affinity, bystander B cells which may be exposed to IL-21 signal as they traverse the vicinity of Tfh cells.

Findings presented in this study also revealed novel insights into the synergy between IL-21 and CD40L. Although we observed a steady increase in IL-21R mRNA in Ly7 cells treated with IL-21 and CD40L (Supplementary Fig. 2), no apparent change was detected at the protein level after 16–24 h (Fig. 4*A*). Nevertheless, CD40L priming greatly enhanced the expression of IL-21R on the cell surface (Fig. 4*C*), which may explain the heightened initial IL-21 response. The much prolonged duration of Jak/STAT3 signaling, however, is unlikely to be caused by the elevated surface IL-21R level *per se*. A more attractive possibility is that CD40L priming triggered down-regulation or physically seclusion of molecules that are normally responsible for the rapid inactivating phase of Jak/STAT signaling, e.g. protein tyrosine phosphatases and the SOCS proteins. In addition to this cell membrane-proximal effect, signals transduced from CD40 and IL-21R also collaborated at the chromatin level to regulate Blimp-1 expression. In this case, the key is competitive binding of BCL6 and STAT3 to the shared intron 3 site in the *PRDM1* locus. Specifically, although CD40L/CD40 did not activate Blimp-1 transcription, it primed the locus for activation by downregulating BCL6 (Fig. 5*C* and Supplementary Fig. S3*B*). In comparison, IL-21 as a single agent activated STAT3 but also increased BCL6 thus sending conflicting signals to the *PRDM1* locus (Fig. 3*A* and ref (41)). Synergy was achieved when STAT3 was optimally loaded to both the 5′s regulatory sites and the intron 3 site under costimulation by both IL-21 and CD40L (Fig. 5*E*).

Transcriptional regulation of Blimp-1 has been intensely investigated with the majority of the published studies focusing on the murine *Prdm1* gene and the 3′ regulatory sequence of this locus (27, 40). In our study, we focused on the shared BCL6/STAT3 site in the human *PRDM1* intron 3 because it is evolutionarily conserved (Supplementary Fig. 3; "site 7" in Kwon et al (42)) and that it is the most critical site mediating the *PRDM1* inhibitory effect of BCL6 in human B cells (9). We note that in the study by Kwon et al (42), STAT3 showed only weak binding to this site in mouse CD4^{+} T cells and this motif did not score functional importance in reporter assays. Reasons for the apparent discrepancy between Kwon et al and our results are unknown, but may be related to cell type and/or species specificity. For IL-21-triggered Blimp-1 upregulation in murine lymphocytes, IRF4 appears to play a critical role. It is preloaded to many STAT3 target genes and guides STAT3 recruitment to these loci upon IL-21 stimulation and STAT3 nuclear translocation (42). IRF4 site (GAAA) occurs quite frequently in the genome. Six IRF4 sites are present in the 300 bp region surrounding the intron 3 BCL6/STAT3 site in human *PRDM1*. Whether any of them is occupied by IRF4 during IL-21 response or IL-21/CD40L costimulation is an issue that can be addressed in future studies.

Lastly, we have validated a robust cell line system that can be used to study the early steps in GC-to-PC phenotypic transition. All the main features we have studied, including the synergy between IL-21 and CD40L, and the importance of STAT3 and Jak3 as signal transducers of IL-21R, are consistent with prior reports in primary human B cells. A limitation of this system is that the phenotypic maturation, as least when induced by IL-21 plus CD40L, likely proceeds only to the pre-PB stage, based on the CD20/CD38 expression pattern and the amount of antibodies secreted (Fig. 2). A possible explanation lies in Pax5,

which should be completely turned off in mature PCs yet declined very slowly under our costimulation condition (Fig. 3*A* and Supplementary Fig. 2). Furthermore, J chain and the spliced form of XBP-1 (XBP-1S), two target genes of Pax5-mediated transcriptional repression, also changed little during the first two days of CD40L/IL-21 co-culture (Supplementary Fig. 2). Nevertheless, compared to the primary GC B cell culture, this Ly7-based system is much more amenable to detailed biochemical and molecular characterizations as demonstrated in this report. In summary, we have characterized a new cell line-based system for *in vitro* studies of GC-to-PC transition. Our experiments based on this system and primary tonsillar GC B cells not only highlighted a critical requirement for STAT3 at the transitional junction between activated centrocyte to pre-PB, but also provided novel and important insights into the synergy between IL-21 and CD40L during PC differentiation.

Supplementary Material

Refer to Web version on PubMed Central for supplementary material.

Acknowledgments

ABBREVIATIONS

|	
Ig	immunoglobulin
PC	plasma cell
ChIP	chromatin immunoprecipitation
PB	plasmablast
DLBCL	diffuse large B cell lymphoma
Pre-PB	pre-plasmablast
GC	germinal center
Tfh	T follicular helper

References

1. Shapiro-Shelef M, Calame K. Regulation of plasma-cell development. Nat Rev Immunol. 2005; 5:230–242. [PubMed: 15738953]

2. Oracki SA, Walker JA, Hibbs ML, Corcoran LM, Tarlinton DM. Plasma cell development and survival. Immunol Rev. 2010; 237:140–159. [PubMed: 20727034]

3. Kallies A, Hasbold J, Fairfax K, Pridans C, Emslie D, McKenzie BS, Lew AM, Corcoran LM, Hodgkin PD, Tarlinton DM, Nutt SL. Initiation of plasma-cell differentiation is independent of the transcription factor Blimp-1. Immunity. 2007; 26:555–566. [PubMed: 17509907]

4. O'Connor BP, Gleeson MW, Noelle RJ, Erickson LD. The rise and fall of long-lived humoral immunity: terminal differentiation of plasma cells in health and disease. Immunol Rev. 2003; 194:61–76. [PubMed: 12846808]

5. Goodnow CC, Vinuesa CG, Randall KL, Mackay F, Brink R. Control systems and decision making for antibody production. Nat Immunol. 2010; 11:681–688. [PubMed: 20644574]

6. Fornek JL, Tygrett LT, Waldschmidt TJ, Poli V, Rickert RC, Kansas GS. Critical role for Stat3 in T-dependent terminal differentiation of IgG B cells. Blood. 2005; 107:1085–1091. [PubMed: 16223771]

7. Ding BB, Yu JJ, Yu RY, Mendez LM, Shaknovich R, Zhang Y, Cattoretti G, Ye BH. Constitutively activated STAT3 promotes cell proliferation and survival in the activated B-cell subtype of diffuse large B-cell lymphomas. Blood. 2008; 111:1515–1523. [PubMed: 17951530]

8. Tunyaplin C, Shaffer AL, Angelin-Duclos CD, Yu X, Staudt LM, Calame KL. Direct repression of prdm1 by Bcl-6 inhibits plasmacytic differentiation. J Immunol. 2004; 173:1158–1165. [PubMed: 15240705]

9. Parekh S, Polo JM, Shaknovich R, Juszczynski P, Lev P, Ranuncolo SM, Yin Y, Klein U, Cattoretti G, Dalla Favera R, Shipp MA, Melnick A. BCL6 programs lymphoma cells for survival and differentiation through distinct biochemical mechanisms. Blood. 2007

10. Basso K, Saito M, Sumazin P, Margolin AA, Wang K, Lim WK, Kitagawa Y, Schneider C, Alvarez MJ, Califano A, Dalla-Favera R. Integrated biochemical and computational approach identifies BCL6 direct target genes controlling multiple pathways in normal germinal center B cells. Blood. 2010; 115:975–984. [PubMed: 19965633]

11. Ci W, Polo JM, Cerchietti L, Shaknovich R, Wang L, Yang SN, Ye K, Farinha P, Horsman DE, Gascoyne RD, Elemento O, Melnick A. The BCL6 transcriptional program features repression of multiple oncogenes in primary B-cells and is deregulated in DLBCL. Blood. 2009

12. Cattoretti G, Chang CC, Cechova K, Zhang J, Ye BH, Falini B, Louie DC, Offit K, Chaganti RS, Dalla-Favera R. BCL-6 protein is expressed in germinal-center B cells. Blood. 1995; 86:45–53. [PubMed: 7795255]

13. Crotty S. Follicular helper CD4 T cells (TFH). Annu Rev Immunol. 2011; 29:621–663. [PubMed: 21314428]

14. Victora GD, Schwickert TA, Fooksman DR, Kamphorst AO, Meyer-Hermann M, Dustin ML, Nussenzweig MC. Germinal center dynamics revealed by multiphoton microscopy with a photoactivatable fluorescent reporter. Cell. 2010; 143:592–605. [PubMed: 21074050]

15. Allen CD, Okada T, Tang HL, Cyster JG. Imaging of germinal center selection events during affinity maturation. Science. 2007; 315:528–531. [PubMed: 17185562]

16. Kosco-Vilbois MH. Are follicular dendritic cells really good for nothing? Nat Rev Immunol. 2003; 3:764–769. [PubMed: 12949500]

17. Haynes NM. Follicular associated T cells and their B-cell helper qualities. Tissue Antigens. 2008; 71:97–104. [PubMed: 18201361]

18. Saito M, Gao J, Basso K, Kitagawa Y, Smith PM, Bhagat G, Pernis A, Pasqualucci L, Dalla-Favera R. A signaling pathway mediating downregulation of BCL6 in germinal center B cells is blocked by BCL6 gene alterations in B cell lymphoma. Cancer Cell. 2007; 12:280–292. [PubMed: 17785208]

19. Linterman MA, Beaton L, Yu D, Ramiscal RR, Srivastava M, Hogan JJ, Verma NK, Smyth MJ, Rigby RJ, Vinuesa CG. IL-21 acts directly on B cells to regulate Bcl-6 expression and germinal center responses. J Exp Med. 2010; 207:353–363. [PubMed: 20142429]

20. Zotos D, Coquet JM, Zhang Y, Light A, D'Costa K, Kallies A, Corcoran LM, Godfrey DI, Toellner KM, Smyth MJ, Nutt SL, Tarlinton DM. IL-21 regulates germinal center B cell differentiation and proliferation through a B cell-intrinsic mechanism. J Exp Med. 2010; 207:365–378. [PubMed: 20142430]

21. Kim HS, Zhang X, Choi YS. Activation and proliferation of follicular dendritic cell-like cells by activated T lymphocytes. J Immunol. 1994; 153:2951–2961. [PubMed: 7522246]

22. Lane P, Brocker T, Hubele S, Padovan E, Lanzavecchia A, McConnell F. Soluble CD40 ligand can replace the normal T cell-derived CD40 ligand signal to B cells in T cell-dependent activation. J Exp Med. 1993; 177:1209–1213. [PubMed: 7681469]

23. Liu YJ, Barthelemy C, de Bouteiller O, Arpin C, Durand I, Banchereau J. Memory B cells from human tonsils colonize mucosal epithelium and directly present antigen to T cells by rapid up-regulation of B7-1 and B7-2. Immunity. 1995; 2:239–248. [PubMed: 7535180]

24. Good KL V, Bryant L, Tangye SG. Kinetics of human B cell behavior and amplification of proliferative responses following stimulation with IL-21. J Immunol. 2006; 177:5236–5247. [PubMed: 17015709]

25. Vasanwala FH, Kusam S, Toney LM, Dent AL. Repression of AP-1 function: a mechanism for the regulation of Blimp-1 expression and B lymphocyte differentiation by the B cell lymphoma-6 protooncogene. J Immunol. 2002; 169:1922–1929. [PubMed: 12165517]

26. Mendez LM, Polo JM, Yu JJ, Krupski M, Ding BB, Melnick A, Ye BH. CtBP is an essential corepressor for BCL6 autoregulation. Mol Cell Biol. 2008; 28:2175–2186. [PubMed: 18212045]

27. Kuo TC, Shaffer AL, Haddad J Jr, Choi YS, Staudt LM, Calame K. Repression of BCL-6 is required for the formation of human memory B cells in vitro. J Exp Med. 2007; 204:819–830. [PubMed: 17403935]

28. Choe J, Choi YS. IL-10 interrupts memory B cell expansion in the germinal center by inducing differentiation into plasma cells. Eur J Immunol. 1998; 28:508–515. [PubMed: 9521060]

29. Arpin C, Dechanet J, Van Kooten C, Merville P, Grouard G, Briere F, Banchereau J, Liu YJ. Generation of memory B cells and plasma cells in vitro. Science. 1995; 268:720–722. [PubMed: 7537388]

30. Cattoretti G, Shaknovich R, Smith PM, Jack HM, Murty VV, Alobeid B. Stages of germinal center transit are defined by B cell transcription factor coexpression and relative abundance. J Immunol. 2006; 177:6930–6939. [PubMed: 17082608]

31. Mangan JK, Tantravahi RV, Rane SG, Reddy EP. Granulocyte colony-stimulating factor-induced upregulation of Jak3 transcription during granulocytic differentiation is mediated by the cooperative action of Sp1 and Stat3. Oncogene. 2006; 25:2489–2499. [PubMed: 16518416]

32. Avery DT, Deenick EK, Ma CS, Suryani S, Simpson N, Chew GY, Chan TD, Palendira U, Bustamante J, Boisson-Dupuis S, Choo S, Bleasel KE, Peake J, King C, French MA, Engelhard D, Al-Hajjar S, Al-Muhsen S, Magdorf K, Roesler J, Arkwright PD, Hissaria P, Riminton DS, Wong M, Brink R, Fulcher DA, Casanova JL, Cook MC, Tangye SG. B cell-intrinsic signaling through IL-21 receptor and STAT3 is required for establishing long-lived antibody responses in humans. J Exp Med. 2010; 207:155–171. [PubMed: 20048285]

33. Asao H, Okuyama C, Kumaki S, Ishii N, Tsuchiya S, Foster D, Sugamura K. Cutting edge: the common gamma-chain is an indispensable subunit of the IL-21 receptor complex. J Immunol. 2001; 167:1–5. [PubMed: 11418623]

34. Habib T, Senadheera S, Weinberg K, Kaushansky K. The common gamma chain (gamma c) is a required signaling component of the IL-21 receptor and supports IL-21-induced cell proliferation via JAK3. Biochemistry. 2002; 41:8725–8731. [PubMed: 12093291]

35. Bryant VL, Ma CS, Avery DT, Li Y, Good KL, Corcoran LM, de Waal Malefyt R, Tangye SG. Cytokine-mediated regulation of human B cell differentiation into Ig-secreting cells: predominant role of IL-21 produced by CXCR5+ T follicular helper cells. J Immunol. 2007; 179:8180–8190. [PubMed: 18056361]

36. Ettinger R, Sims GP, Fairhurst AM, Robbins R, da Silva YS, Spolski R, Leonard WJ, Lipsky PE. IL-21 induces differentiation of human naive and memory B cells into antibody-secreting plasma cells. J Immunol. 2005; 175:7867–7879. [PubMed: 16339522]

37. Darnell JE. Validating Stat3 in cancer therapy. Nat Med. 2005; 11:595–596. [PubMed: 15937466]

38. Quandt K, Frech K, Karas H, Wingender E, Werner T. MatInd and MatInspector: new fast and versatile tools for detection of consensus matches in nucleotide sequence data. Nucleic Acids Res. 1995; 23:4878–4884. [PubMed: 8532532]

39. Ehret GB, Reichenbach P, Schindler U, Horvath CM, Fritz S, Nabholz M, Bucher P. DNA binding specificity of different STAT proteins. Comparison of in vitro specificity with natural target sites. J Biol Chem. 2001; 276:6675–6688. [PubMed: 11053426]

40. Sciammas R, Shaffer AL, Schatz JH, Zhao H, Staudt LM, Singh H. Graded expression of interferon regulatory factor-4 coordinates isotype switching with plasma cell differentiation. Immunity. 2006; 25:225–236. [PubMed: 16919487]

41. Ozaki K, Spolski R, Ettinger R, Kim HP, Wang G, Qi CF, Hwu P, Shaffer DJ, Akilesh S, Roopenian DC, Morse HC 3rd, Lipsky PE, Leonard WJ. Regulation of B cell differentiation and

plasma cell generation by IL-21, a novel inducer of Blimp-1 and Bcl-6. J Immunol. 2004; 173:5361–5371. [PubMed: 15494482]

42. Kwon H, Thierry-Mieg D, Thierry-Mieg J, Kim HP, Oh J, Tunyaplin C, Carotta S, Donovan CE, Goldman ML, Tailor P, Ozato K, Levy DE, Nutt SL, Calame K, Leonard WJ. Analysis of interleukin-21-induced Prdm1 gene regulation reveals functional cooperation of STAT3 and IRF4 transcription factors. Immunity. 2009; 31:941–952. [PubMed: 20064451]
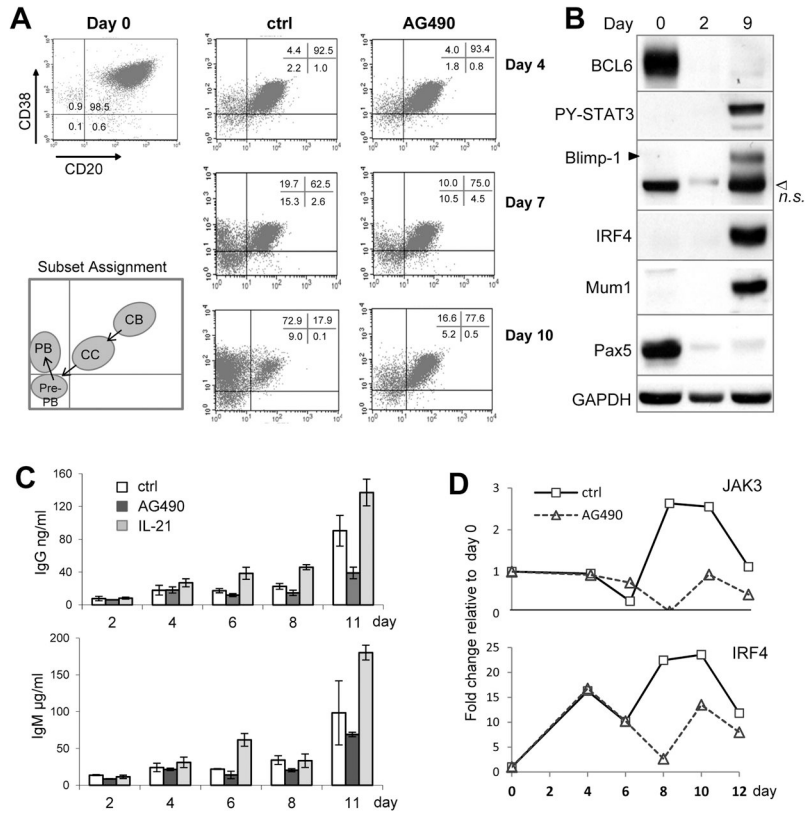
FIGURE 1. STAT3 activation is required for the centrocyte (CC) to pre-plasmablast (Pre-PB) transition of cultured GC B cells

Purified $CD20^{hi}CD38^{hi}$ centroblasts (CB) were differentiated in vitro in the presence of IL-2, IL-4, and CD40L-CD8 fusion on HK cells for 12 days. In parallel cultures, AG490 (5 uM) or IL-21 (50 ng/ml) was included throughout the assay to either inhibit or further activate Jak/STAT signaling, respectively. *A*. On indicated days, aliquots of cells from the control (ctrl) and AG490 cultures were stained and B cell subsets identified based on surface CD20 and CD38 expression. *B.* Changes in the expression of indicated transcription factors were analyzed by Western Blot. n.s., a non-specific band recognized by the polyclonal Blimp-1 Ab. The Mum1 Ab recognizes a conformational epitope on the IRF4 protein enriched in the nucleus (30). GAPDH is used as a loading control. *C.* Culture supernatants were harvested on the days indicated from control, AG490, and IL-21 cultures, and analyzed by ELISA for total IgG and IgM Ab production. Plotted in the graph are mean ± s.d. of two duplicate cultures in the same experiment. Note the different y-axis scale for IgM and IgG. *D.* Expression of *Jak3* and *IRF4* mRNA was measured by qRT-PCR on RNA samples prepared from the control and AG490 cultures on the days indicated. Data are representative of 3 or more independent experiments.
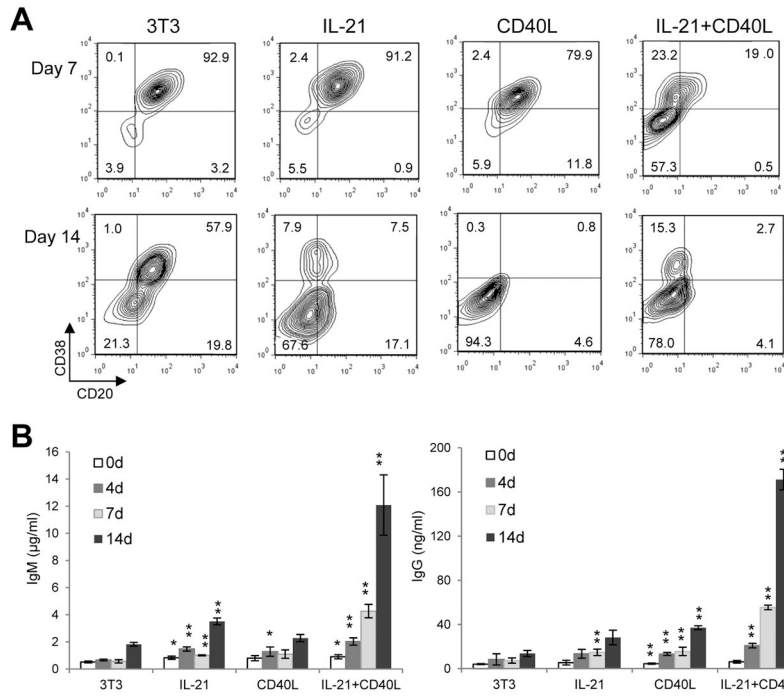
FIGURE 2. The DLBCL cell line Ly7 can be efficiently induced to adopt a PC-like phenotype when costimulated by IL-21 and membrane bound CD40L
Ly7 cells were cultured for 14 days in the presence or absence of IL-21 on either control 3T3 fibroblasts or 3T3-CD40L stable transfectants. *A*. On day 7 and 14, aliquots of cells were stained and phenotypic changes were examined based on CD20 and CD38 expression. *B.* Culture supernatants taken on day 0, 4, 7 and 14 were analyzed by ELISA for production of total IgM and IgG antibodies. Note the different y-axis scale for IgM and IgG. Student t-tests were performed to compare the Ig titer from a given treatment to that of the control culture (3T3) on the same day. *, *P* < 0.05; **, *P* < 0.01. Results are representative of 4 independent experiments.
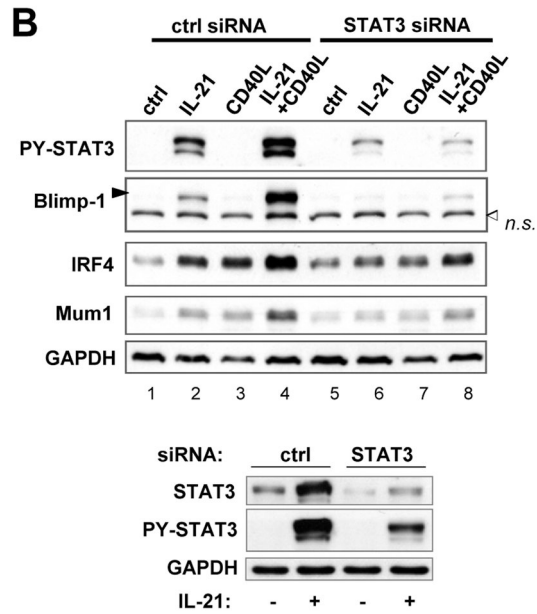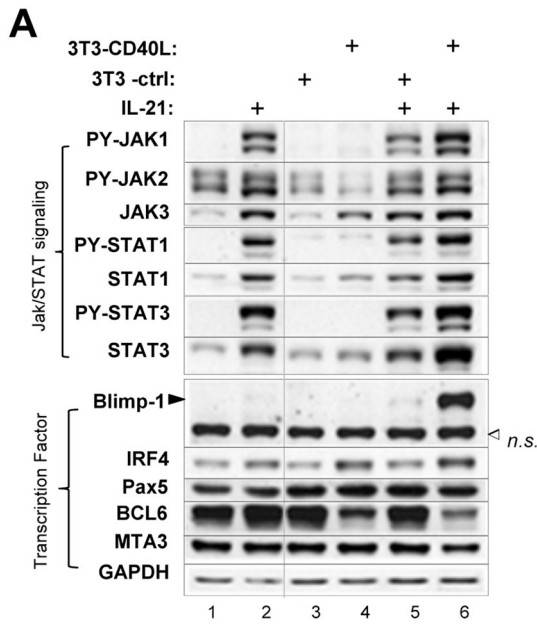
FIGURE 3. IL-21 and CD40L synergistically induce Blimp-1 expression in a STAT3-dependent manner
A. Ly7 cells were subjected to culture conditions as described for Figure 2. After 46 h, whole cell lysates were prepared and analyzed by Western Blot for the expression of indicated protein markers. *B.* Forty-eight hours after being transfected with either control (ctrl) or STAT3-specific siRNA oligos, Ly7 cells were stimulated as indicated for another 44 h. Whole cell lysates were prepared and subject to Western Blot analysis for the indicated protein markers. The RNAi-mediated knock-down effect of total STAT3 protein was shown in the bottom panel. *n.s.*, non-specific band.
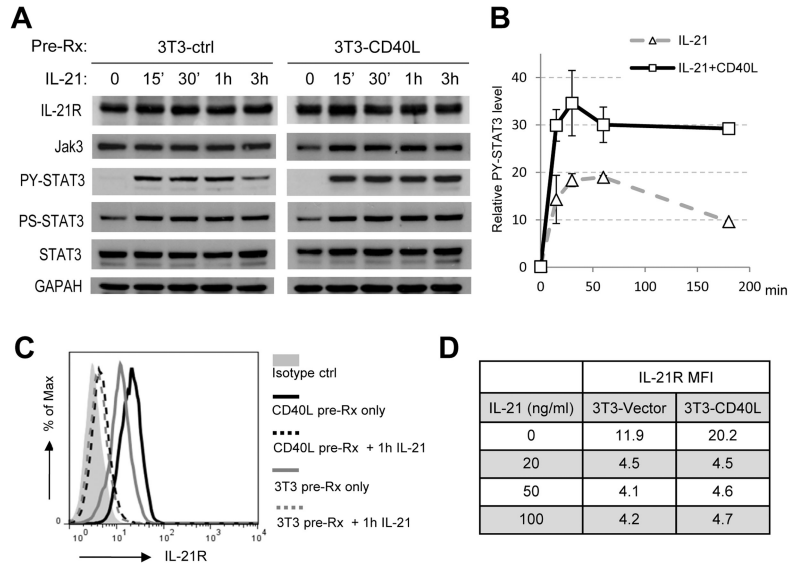
FIGURE 4. Engagement of the CD40 receptor potentiates Jak/STAT3 signaling by upregulating surface IL-21R expression

Ly7 cells were cultured for 16 h on either the control 3T3 (3T3-ctrl) or 3T3-CD40L feeder cells prior to IL-21 stimulation. *A.* Whole cell lysates were prepared at the indicated time points during IL-21 treatment and analyzed by Western Blot for the indicated protein markers. *B.* Normalized intensity of PY-STAT3 bands were plotted against IL-21 treatment time. The graph shows the mean +/− S.D. of two independent experiments. *C–D.* Aliquots of cells that were either untreated or exposed to varying concentrations of IL-21 for 1 h were analyzed for surface IL-21R expression. FACS profiles for untreated cells and those treated with 100 ng/ml IL-21 are shown in *C*. Mean fluorescence intensity (MFI) values for all samples are listed in *D*.
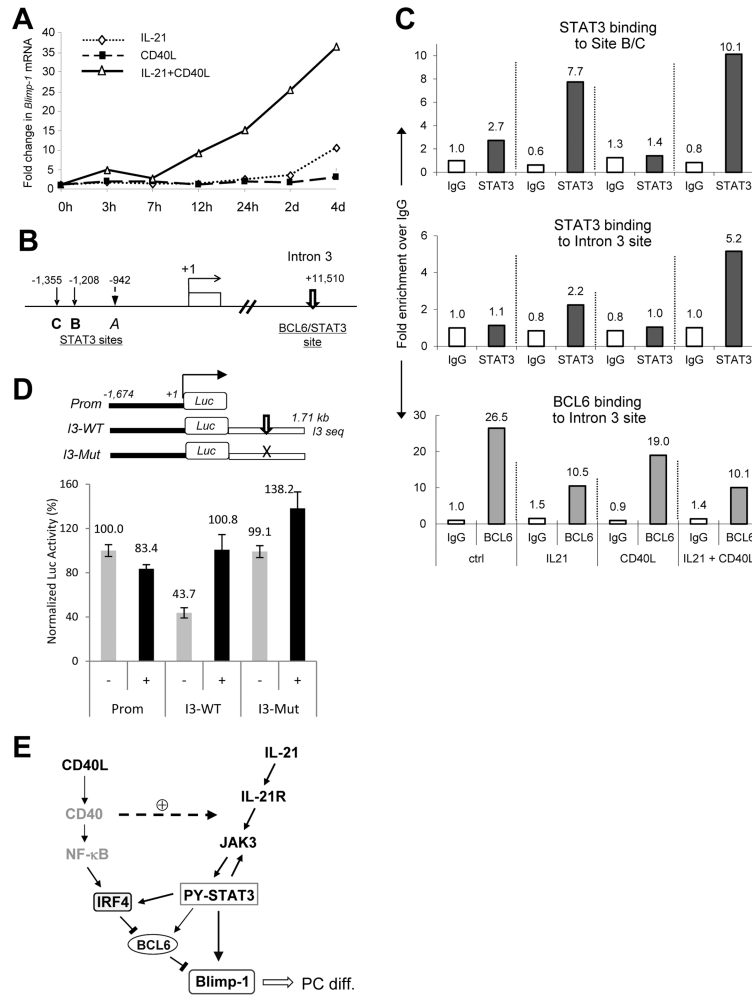
FIGURE 5. CD40L/CD40 binding cooperates with IL-21 to load STAT3 onto the shared BCL6/STAT3 site within intron 3 of the *PRDM1* gene
A. qRT-PCR analysis of *Blimp-1* mRNA in Ly7 cells treated as indicated during a period of 1–4 days. All values were normalized to the pre-treatment level defined as 1.0. *B.* Schematic representation of the 5′ regulatory region of the human *PRDM1* gene and its third intron showing a shared BCL6/STAT3 site. Transcriptional start site +1 is defined as in GenBank accession number AY198414 (http://www.ncbi.nlm.nih.gov/genbank/). Graph is not drawn to scale. *C.* Ly7 cells pretreated with either control or 3T3-CD40L feeder overnight were left either untreated (ctrl and CD40L) or treated with 100 ng/ml IL-21 for 1 h (IL-21 and IL-21+CD40L). Chromatin was cross-linked and purified from cells subjected to different treatment conditions. Binding of endogenous STAT3 and BCL6 to the indicated regions of the *PRDM1* gene were analyzed by qChIP. Signals enrichment by normal rabbit IgG was also measured and used as background control (set as 1.0 in the graphs). *D.* IL-21/CD40L stimulated transcriptional response from the 3 Blimp-1 Luciferase reporters illustrated at the top. Ly7 cells transiently transfected with the reporters were either left untreated or subject to IL-21/CD40L costimulation as in Figure 3. Cells were harvested for reporter assays 44 h later. Plotted in the graph are the means ± SD of duplicate tests with the mean from the untreated promoter only construct set as 100. *E*. A working model depicting regulatory relationships between the signaling molecules and transcriptional factors that we have analyzed in this study. Plain lines with arrow heads represent sequential events or positive

regulation; blunt bars represent negative regulation. The dashed arrow with a circled plus sign depicts a potentiation effect of activated CD40 on IL-21R/Jak/STAT3 signaling. Roles of the molecules in grey, CD40 and NF-κB, are based on published literature. For simplicity, the direct influence of IRF4 on Blimp-1 as well as inhibitory effects of BCL6 on IRF4 and STAT3 are not shown. PC diff., PC differentiation.